Supplemental Material

Copper-Transporting P-Type ATPases utilize a Unique Ion-Release Pathway

Magnus Andersson[1,4,6], Daniel Mattle[2,5,6], Oleg Sitsel[2], Tetyana Klymchuk[2], Anna Marie Nielsen[2], Lisbeth Birk Møller[3], Stephen H. White[1], Poul Nissen[2] & Pontus Gourdon[2]

[1] Department of Physiology and Biophysics, University of California at Irvine, Irvine, USA

[2] Centre for Membrane Pumps in Cells and Disease (PUMPKIN), Danish National Research Foundation, Aarhus University, Department of Molecular Biology and Genetics, Aarhus, Denmark

[3] Applied Human Molecular Genetics, Kennedy Center, Copenhagen University Hospital, Rigshospitalet, Glostrup, Denmark

[4] Magnus Andersson's present address is Science for Life Laboratory, Theoretical and Computational Biophysics, Department of Theoretical Physics, Swedish e-Science Research Center, Royal Institute of Technology (KTH), Solna, Sweden

[5] Daniel Mattle's present address is Laboratory of Biomolecular Research, Paul Scherrer Institut, Villigen, Switzerland

[6] Contributed equally

Correspondence should be addressed to P.G. (pgo@mb.au.dk).

Nature Structural and Molecular Biology: doi:10.1038/nsmb.2721

Figures - Supplementary Figure 1.

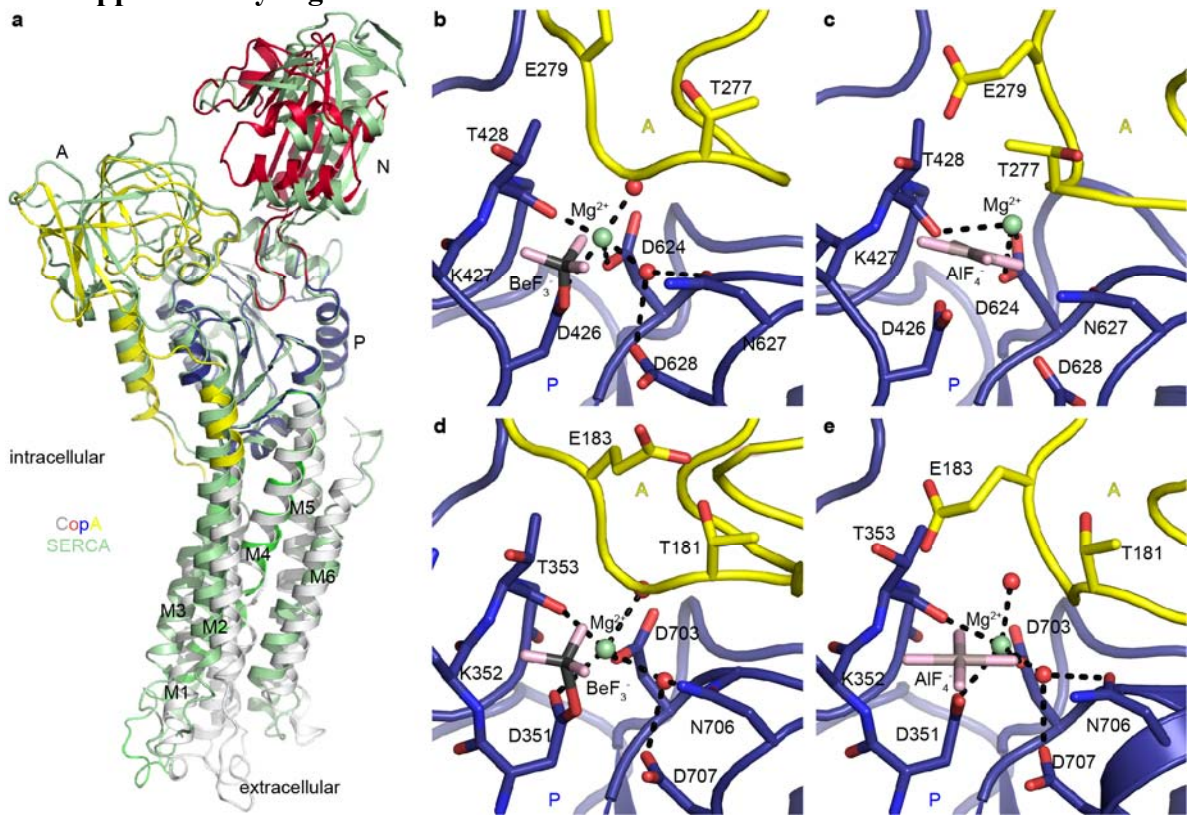

Supplementary Figure 1. **Comparison of the E2.P_i and E2P states of of LpCopA and SERCA. (a)**, Domain arrangements in the E2P states of LpCopA and SERCA. LpCopA is shown as in Fig. 1b and SERCA (pdb-id: 3B9B[13]) in green. Superimpositions were made of the intracellular domains using super in PYMOL. TM helices MA and MB, M7-M10 as well as SERCA insertions have been removed for clarity. (**b-e**), Close-up view of the phosphorylation site of LpCopA and SERCA. The A- and P-domains (LpCopA and SERCA) are indicated by colors as in Fig. 1a and the catalytic aspartate (Asp426 in LpCopA) and selected residues important for (de)phosphorylation are shown as sticks. (**b**), The E2P state in complex with BeF_3^- (Be in black, F in pink) and the Mg^{2+} ion (green) associated with Asp426. (**c**), The subsequent (forward reaction) E2.P_i conformation with AlF_4^- (Al in brown, F in pink) and the Mg^{2+} ion (green) associated with Asp426 (pdb-id: 3RFU[18]). Note the shift in the position of the A-domain relative to the P-domain between the conformations. (**d**), Equivalent view as in (b) for the E2P state of SERCA (pdb-id: 3B9B[13]). (**e**), Equivalent view as in (c) for the E2.P_i state of SERCA (pdb-id: 3B9R[13]).

Figures – Supplementary Figure 2

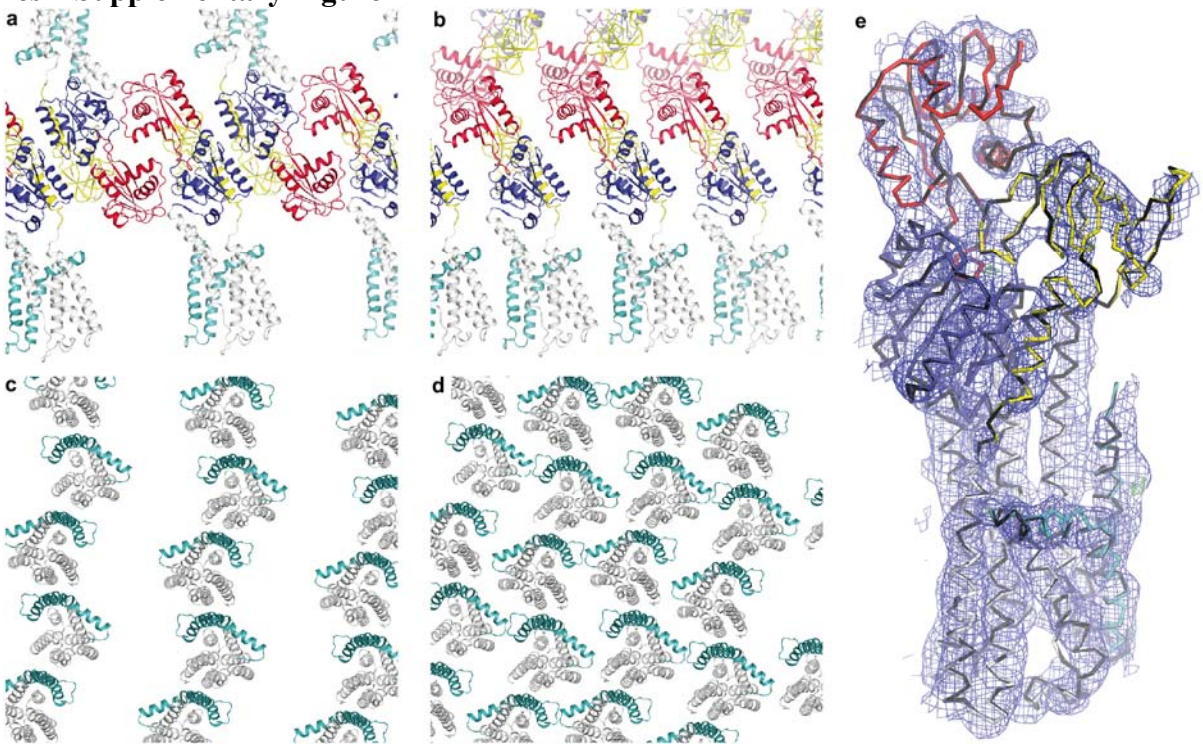

Supplementary Figure 2. Two E2P crystal forms of LpCopA. (**a-d**), Crystal packing with the domains are colored as in Fig. 1b. The proteins are arranged as stacked bilayers, held together by hydrophobic interactions between their membrane-spanning regions, typical of the HiLiDe crystallization method[41]. (**a**), View along the membrane bilayer for the C2 (high-resolution) crystal form. (**b**), Equivalent view for the $P2_12_12_1$ crystal form. Approximate perpendicular views of (a) and (b) are shown in (**c**) and (**d**), respectively. Note the more loose packing of the C2 lattice. The unit cell parameters can be found in Table 1. (**e**), Electron density maps of the low resolution $P2_12_12_1$ form of the E2-BeF_3^- complex. The search model is based on the high-resolution structure (C2 space group) and is colored as in Fig. 1b. The 2mFo-DFc (blue, 1σ contour level) and mFo-DFc (±4σ contour levels, green and red, respectively) electron density maps were derived upon rigid body refinement and indicate no major deviations from the high-resolution structure

Figures – Supplementary Figure 3

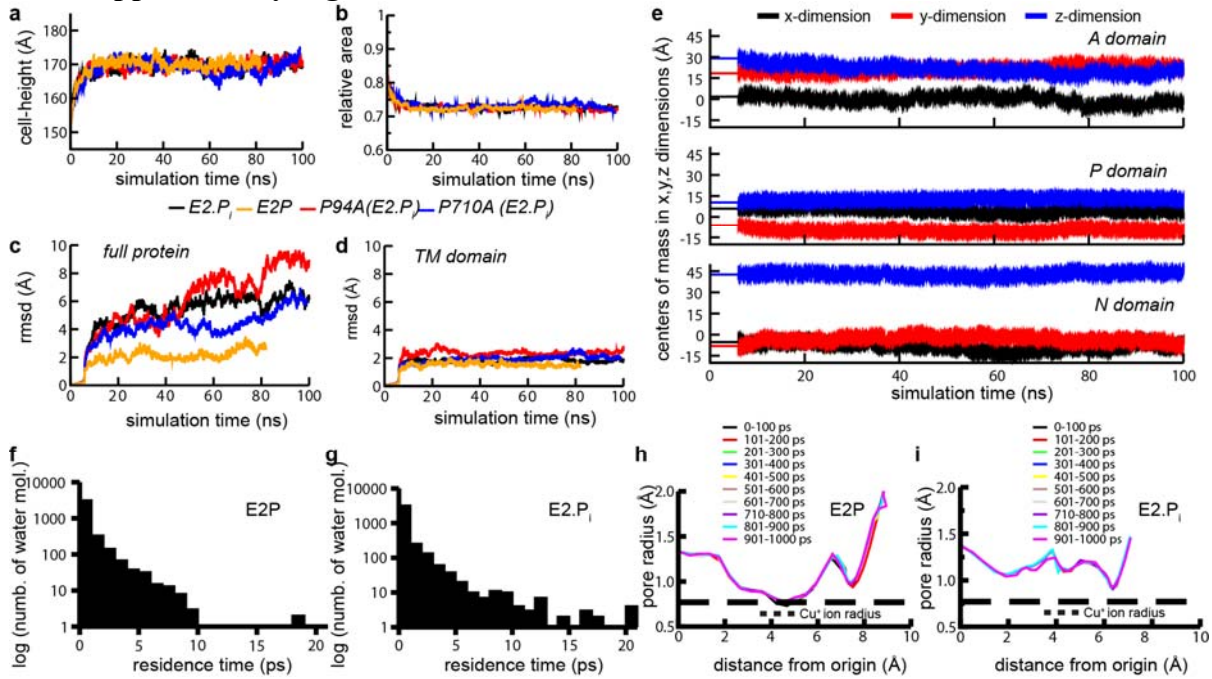

Supplementary Figure 3. MD Simulation Analyses. (**a**), Evolution of the simulation box cell height. (**b**), The corresponding relative cell area (X,Y) evolution. (**c-d**), Backbone RMSD measured over the MD trajectory for states E2.P_i and E2P, and E2.P_i mutants P94A and P710A in the full protein (**c**) and the TM domain (**d**). (**e**), Centers of mass in x, y and z dimensions of the intracellular domains during the E2.P_i simulation. (**f-g**), Residence times for water molecules within 7 Å of Glu189 associated with the release pathway in the E2.P_i (**f**) and E2P (**g**) simulations. Two crystal waters remained associated with the internal water pockets within the release pathway for the entire E2P simulation and hence have residency times of 85 ns (not included in (f)). (**h-i**), Radii analyses. To determine structural variations of the release pathway within the 10 ns average from the MD simulations presented in Fig. 3d, the last 10 ns of the E2P (**h**) and E2.P_i (**i**) simulations were divided into 10 equally spaced 100 ps averages and subjected to Caver analyses.

Figures – Supplementary Figure 4

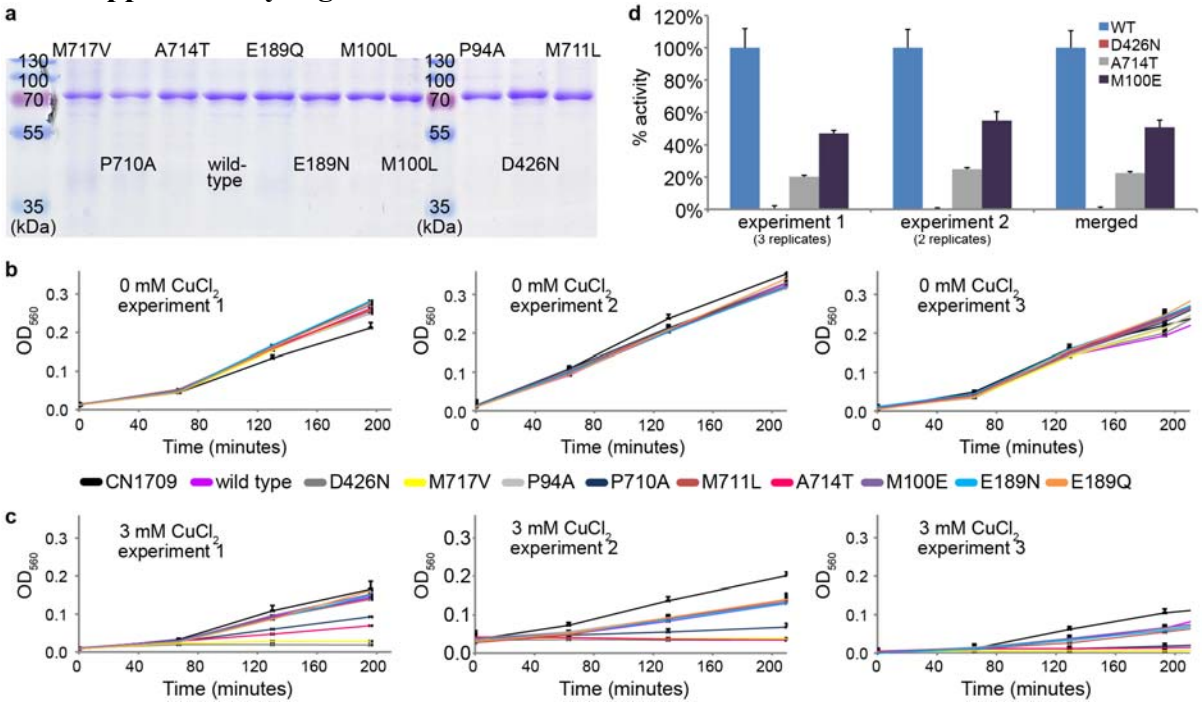

Supplementary Figure 4. Functional analysis of mutant LpCopA forms. (**a**), Purity of the assayed constructs used for the *in vitro* assay. SDS-PAGE gels of the purified LpCopA constructs following a first round of scaling using ImageJ. Identical relative amounts of protein were used for the Baginski assay[25] for generating the raw data shown in Supplementary Table 1. (**b-c**), The *in vivo* copper susceptibility assay. *E. coli* growth complementation curves from three independent experiments for wild-type LpCopA (WT, red), the inactive Asp426Asn mutant (gray), the high-affinity coordinator mutant Met717Val (yellow) as well as various release pathway mutants are displayed. Experiments 1 and 3 used three replicates each, experiment 2 used 15 replicates. 0 and 3 mM copper ((**b**) and (**c**), respectively) were used in the growth medium. (**d**), Assessment of the reproducibility of the *in vitro* assay. The *in vitro* data shown in Fig. 4c are based on a single experiment (experiment 1, with nine replicates), so wild type, Asp426Asn, Ala714Thr and Met100Glu LpCopA were reproduced in additional experiments (experiment 2, with six replicates). The two independent sets of data are highly consistent (merged data).

Figures – Supplementary Figure 5

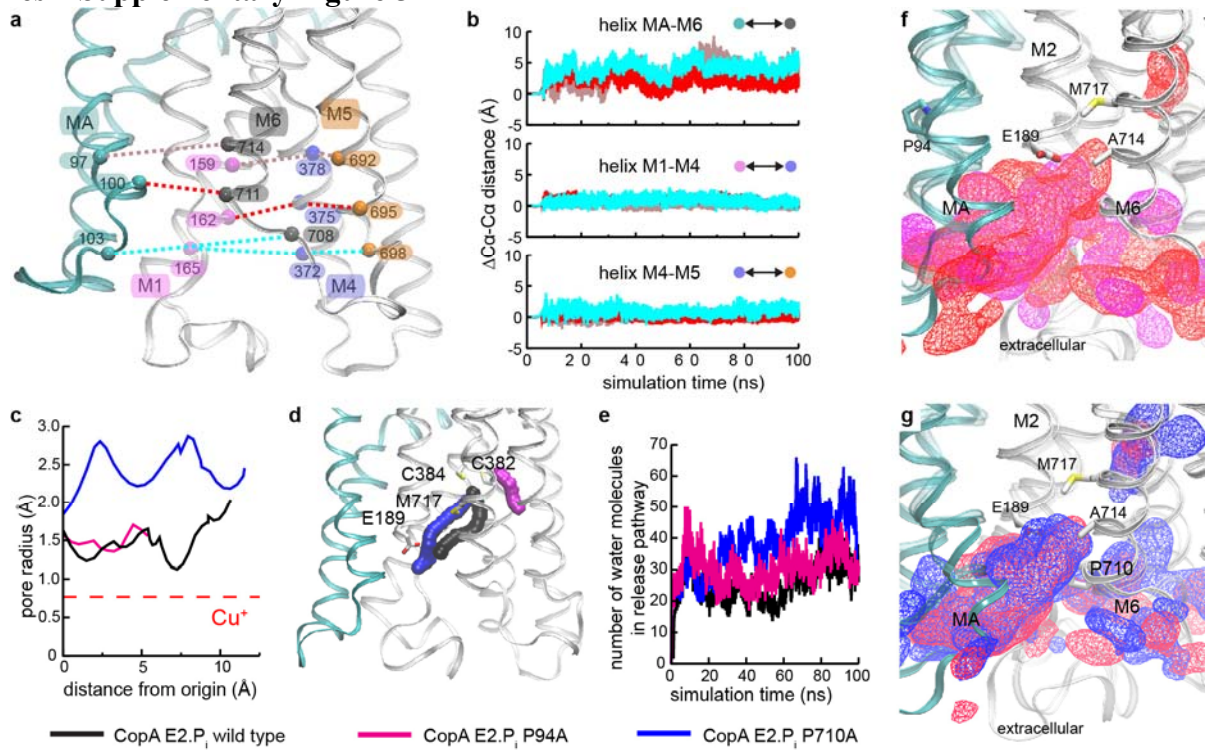

Supplementary Figure 5. Support of a proline-dependent opening mechanism. (**a-b**), Helix dynamics in the E2.P_i simulation with LpCopA colored as in Fig. 1b. (**a**), Calculated inter-helical distances with spheres indicating Cα atoms. Three equally interspersed distances (along the normal to the membrane) in the TM domain were measured for each TM helix pair; gray (intracellular end), red and cyan (extracellular end) dotted lines between helices MA:M6, M1:M4 and M4:M5. (**b**), The helix-pair distances in (a) plotted as gray (intracellular end), red and cyan (extracellular end) lines. (**c-g**), Altered hydration patterns for simulations of the Pro94Ala (purple) and Pro710Ala (blue) mutants compared to wild-type (black). (**c**), Pore radius analyses of average structures from the E2.P_i simulations. (**d**), Structural representation of the pores predicted by CAVER. (**e**), Number of water molecules associated with the release pathway. (**f**), Average representations from the simulations of wild type (solid) and the Pro94Ala mutant (transparent) with the side chains of Pro94, Met717 and Glu189 pinpointed. Water is shown as red (wild type) and green (mutant) iso-density surfaces at 22 % occupancy. (**g**), Equivalent view as in (f) for wild type (solid, red water) and the Pro710Ala mutant (transparent, blue water).

Figures – Supplementary Figure 6

Supplementary Figure 6. Sequence and secondary structure conservation of the P_{IB-1}-, P_{IB-2}- and P_{IB-4}-ATPases. (**a**), Alignment and sequence conservation of three representative members of the P_{IB-1}-, P_{IB-2}- and P_{IB-4}-ATPases. The sequences used have locus tags lpg1024 (CopA), JW3434 (ZntA) and msmeg_5403 (CtpD). For analysis of conservation level, the ConSurf server was used[72]. Determination of conservation was based on 617 sequences having a sequence identity below 95% for P_{IB-1}-ATPases, 520 sequences below identity=99% for P_{IB-2}-ATPases and 607 sequences below identity=99% for P_{IB-4}-ATPases. Information from (b) was used for adjusting the alignments of helices MA and MB due to poor sequence conservation in this region. The black box indicates the position of Pro94 in LpCopA. (**b**), Secondary structure based alignment of the N-terminal segment of the ATPase core of P_{IB-1}-, P_{IB-2}- and P_{IB-4}-ATPases. Ten weakly redundant members of each subgroup were selected and aligned based on secondary structure prediction using the PSIPRED server[73]. Only the region from the start of helix MA to MB' is shown. The UniProtKB entries of the sequences are indicated to the left. Highlighted in bold are first sequences in each subgroup which are also used in (a).

Tables - Supplementary Table 1.

a

WT	D426N	M717V	P94A	P710A	M711L	A714T	M100L	M100E	E189N	E189Q
1.483	0.393	0.358	0.615	0.355	0.637	0.492	1.130	0.743	0.564	0.805
1.466	0.389	0.357	0.603	0.351	0.631	0.498	1.141	0.700	0.568	0.817
1.308	0.362	0.322	0.582	0.338	0.565	0.474	1.020	0.729	0.533	0.732
1.479	0.393	0.342	0.615	0.337	0.642	0.503	1.121	0.758	0.533	0.886
1.395	0.388	0.360	0.596	0.342	0.662	0.507	1.155	0.768	0.540	0.921
1.588	0.368	0.319	0.632	0.329	0.626	0.501	1.080	0.758	0.519	0.874
1.649	0.336	0.330	0.588	0.315	0.598	0.481	1.148	0.784	0.564	0.942
1.659	0.373	0.340	0.588	0.317	0.599	0.496	1.148	0.752	0.557	0.910
1.708	0.338	0.322	0.534	0.291	0.547	0.480	1.100	0.770	0.511	0.796
Averages:										
1.526	0.371	0.339	0.595	0.331	0.612	0.492	1.116	0.751	0.543	0.854
Normalized to WT (100%) and D426N (0%):										
100%	0%	-3%	19%	-4%	21%	11%	64%	33%	15%	42%

b

WT	D426N	M717V	P94A	P710A	M711L	A714T	M100L	M100E	E189N	E189Q
Integrated band intensities:										
7722675	8637304	5480970	6723758	4578525	7638705	6626940	6654735	6480825	6877605	7787190
Signal scaling factor:										
0.894	1.000	0.635	0.778	0.530	0.884	0.767	0.770	0.750	0.796	0.902
Raw averages:										
1.526	0.371	0.339	0.595	0.331	0.612	0.492	1.116	0.751	0.543	0.854
Scaled averages:										
1.707	0.371	0.534	0.764	0.624	0.692	0.642	1.448	1.001	0.682	0.947
Normalized to WT (100 %) and D426N (0 %), based on scaled averages:										
100 %	0 %	12 %	29 %	19 %	24 %	20 %	81 %	47 %	23 %	43 %

Supplementary Table 1. **The *in vitro* data.** (**a**), Raw data from the activity measurements. The averaged values have been calculated and, finally, the scaled data where the background, the absorbance measured for the D426N dead mutant, has been removed and then divided with the average absorbance for the wild type (WT). (**b**), Process for obtaining the data displayed in Fig. 4c. The LpCopA bands from the SDS-PAGE (Supplementary Fig. 4a) were quantified using ImageJ by calculating their integrated band intensities. This allowed a scaling factor to be derived, by which the raw absorbance signal averages were divided in order to obtain the scaled absorbance averages. The final data were computed by removing the background, the absorbance measured for the D426N dead mutant, and then divide the resulting background compensated values with the average absorbance for the wild type (WT).

Supplementary References

72. Ashkenazy, H., Erez, E., Martz, E., Pupko, T. & Ben-Tal, N. ConSurf 2010: calculating evolutionary conservation in sequence and structure of proteins and nucleic acids. *Nucleic Acids Res* **38**, W529-33 (2010).

73. Buchan, D.W. et al. Protein annotation and modelling servers at University College London. *Nucleic Acids Res* **38**, W563-8 (2010).